Direct Determination of Gray Participating Thermal Radiation Properties of Insulating Materials

A. Saboonchi,* W. H. Sutton,† and T. J. Love‡
University of Oklahoma, Norman, Oklahoma

A technique for the unique determination of the scattering coefficient and mass extinction coefficient of insulation in infrared wavelengths is developed. Measurement of actual transmission and reflectance is made and compared with the isotropic scattering model so that the values reported are *effective properties* suitable for use in gray isotropic scattering analyses. An experimental apparatus is devised in which transmitted and reflected components of a diffuse incident flux on an insulation specimen have been measured, and the results are compared to an analysis of isotropic scattering with diffuse boundaries using Case's normal mode expansion method to determine the property values. Experimental measurements were made on four different brands of glass-fiber insulation, three kinds of Fiberfrax (silica fiber) insulation, and two different brands of foam insulation. Because of the random distribution of fibers, measurements were made with different densities in order to provide statistical averages of the properties.

Introduction

LOW-DENSITY thermal insulating materials, which provide considerable savings of cost, space, and weight, are utilized in many heat-transfer applications. These materials are being used extensively in consumer appliances, homes, industrial process equipment, automobiles, and aircraft. Radiative transport becomes important for high-temperature applications such as flame barriers. It is also important in high-altitude, low-pressure applications.

The effectiveness of thermal insulation is usually determined using the guarded hot-box method,[1] which gives an apparent thermal conductivity. However, because thermal conduction is ordinarily not the primary mode of heat transfer in these materials, at higher temperatures, such measurements are of limited utility. It is desirable to determine actual material properties in order to allow for a more accurate analysis in critical design applications and to allow rapid evaluation of new insulating materials.

To account properly for radiation in such materials, the properties of the bounding surfaces, their absolute temperature, and the radiative properties of the insulation must be known. In the prediction of radiative transfer between surfaces, diffuse reflectance is usually assumed. Further, the detailed scattering characteristics (phase function and dependent scattering model) are difficult, if not impossible, to obtain for random fiber insulation. Previously published analytical studies of radiative transport with multiple scattering assume axially symmetric scattering functions. Fibrous insulation will not scatter in an axially symmetric fashion because of the anisotropic orientation of the fibers. Just as in usual radiation computations, an isotropic analysis is a useful and practical method of estimating the radiative transfer. Even this has not been possible previously because measured values of the albedo and the extinction coefficients have not been available without significant analytical approximation of the scattering.

Analytical techniques[2-15] have been proposed for determining the coupled conduction, convection, and radiation heat transfer in thermal insulation. The major difficulty with these analyses is that the radiative properties of such materials are very difficult to determine and are generally unknown. More recent work[7] indicates that gray isotropic properties are sufficient for assessing media and boundary effects in one-dimensional combined mode problems.

In most materials, the inhomogeneities or particles are not widely spaced relative to the size of the scattering defect so that one may not use a distribution function with the applicable single scattering model to determine the radiative properties. The scattering coefficient may be determined theoretically based on particle size and refractive index[5] for clouds of widely separated particles; however, such analysis is not generally applicable to packed insulation materials. For the case of glass-fiber insulation, the medium is manufactured by randomly building up successive layers of fibers treated with a resin binder until the desired thickness is achieved. This process causes two major measurement difficulties.

1) It is difficult to construct a statistically meaningful optically thin sample because of the grossly random distribution of the fibers. Additionally, the fiber orientation and finish could be disturbed in the attempt to construct such a sample.

2) The material will exhibit dependent scattering as a result of the fibers actually touching in many places.

An optically thick sample, while statistically suitable, leads to uniqueness problems in correlating the transmitted normal intensity to an extinction coefficient. That is to say, different combinations of albedo and extinction coefficient may result in the same transmittance. An example of this behavior is shown in Fig. 1. Transmittance is plotted for two albedos and two typical extinction coefficients over a range of specimen density thicknesses. The overlap of values is readily apparent.

The current experimental study has overcome the aforementioned difficulty and demonstrates a method for uniquely determining the albedo and extinction coefficients for insulating materials. In this experimental arrangement, the measurement of both transmitted and reflected components of a diffuse incident flux on an insulation specimen have been made, and the results are presented. The analytical correlation was developed using the normal mode expansion method of solution for radiative transport.

Review of Related Literature

Verschoor and Greebler[13] measured thermal conductivity of glass-fiber insulation and considered thermal radiation as acting on successive plates of fibers perpendicular to the direction of heat flow. The heat energy received by the main

Received Nov. 14, 1986; revision received April 16, 1987.

*School of Aerospace, Mechanical, and Nuclear Engineering.
†Assistant Professor, Aerospace, Mechanical and Nuclear Engineering.
‡George Lynn Cross and Haliburton Professor, Aerospace, Mechanical and Nuclear Engineering; Interim Dean, College of Engineering. Associate Fellow AIAA.

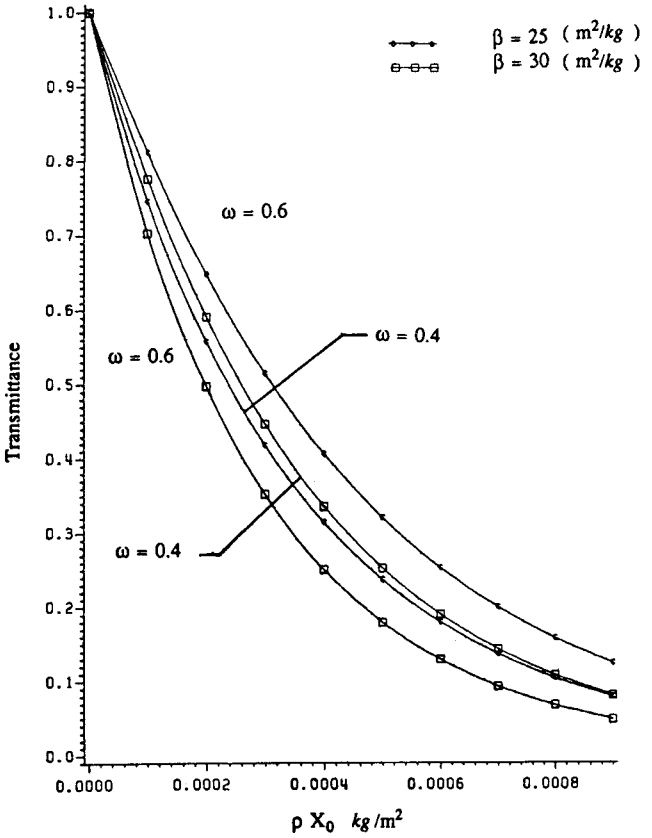

Fig. 1 Uniqueness difficulties for transmittance measurements.

plane, from all other planes close to a hot plate surface, was evaluated using the Stefan-Boltzmann radiation law. In this model, no consideration was given to scattering or extinction coefficients of the glass fiber insulation.

Larkin and Churchill[5] investigated, both theoretically and experimentally, radiant transfer through fibers and foamed insulating materials. Transmission measurements were made under isothermal conditions with a blackbody source varying from 200 to 800°F (93.3–426.7°C). Density, fiber, and pore size were also varied. Scattering and extinction coefficients were not evaluated.

Hager and Steere[3] derived expressions for calculating radiant-heat-transfer rates in laminar arrays of high-emissivity fibers having diameters much larger than the wavelength of emitted radiation. A model was devised to calculate radiation heat transfer in fibrous thermal insulation, assuming that the voids between fibers are either evacuated or filled with gas at atmospheric pressure. Thermal conductivity of glass-fiber insulation was calculated at the mean sample temperature of about 303 K at different pressures. Reflection, diffraction, and radiant transmission phenomena were neglected.

Tong and Tien[11,12] have done extensive analytical and experimental work to calculate radiative heat transfer in glass-fiber insulation. Analytically, the two-flux solution of heat transfer is used[11] for isotropic scattering and later work[12] for linear anisotropic scattering. The extinction coefficient was calculated assuming independent single scatter using Beer's law[16] to correlate normal transmittance measurements. While Beer's law approximates the measurement of optical properties of gases with optically thin suspensions of nonconducting particles, glass-fiber insulation consists of poorly conducting filaments that may be closely spaced or touching. Because the transmissivity measurements yield only the extinction coefficient, an analytical value for albedo, ω, was determined from single scattering theory. Finally, Tong et al.[16] used the guarded hot-plate method to measure heat transfer. In more recent work, Tong et al.[17] considered the effects of multiple scatter by using an artificial scaling factor to identify the deviation from Beer's law.

Chan[2] also determined the extinction coefficient β, using Beer's law. Again, the scattering coefficient was not experimentally determined.

Love and Saboonchi[18] and Saboonchi[19,20] measured the normal transmittance in glass fiber insulation and found that the results were not repeatable unless the optical thickness was greater than about 2.6. The spectral mass extinction coefficient was then determined using Beer's law; very little deviation from the gray body assumption was observed. It was recognized that the effects of *in scattering* were not accounted for in this work. However, measurements were made over a range of optical thickness in order to note this effect. The average value of β from those experiments must be considered only approximate and should not be used for accurate predictions.

Analysis

If the glass-fiber insulation sample is assumed to be a uniform, isotropically scattering, plane-parallel slab of physical thickness X_0, the monochromatic radiative intensity may be determined from the solution to the radiative transfer equation

$$\mu\frac{\partial I(\tau,\mu)}{\partial\tau}+I(\tau,\mu)=\frac{\omega}{2}\int_{-1}^{1}I(\tau,\mu')\mathrm{d}\mu' \qquad (1)$$

where

$\omega=\sigma/\beta$ is the scattering albedo

τ = the optical variable, defined by $\mathrm{d}\tau=\rho\beta\mathrm{d}X$

$\tau_0=\rho\beta X_0$ is the optical thickness of the slab; X_0 is the slab thickness

$\mu=\cos\Theta$; Θ defines the angle of propagation of the radiation with respect to the surface normal of the material. Since the surface of insulation is poorly defined, X_0 is difficult to measure directly. However, the quantity ρX_0 for the slab may be determined accurately by measuring the mass and dividing by the relatively large planar area. The mass extinction coefficient β is determined instead of the volumetric coefficient $\rho\beta$, which is typically used analytically but is not a material property, because the density of the insulation may vary with compression or packing.

The boundary conditions used for the solution to this radiation problem are governed by the sample plus the experimental setup illustrated in Fig. 2. Each surface of the

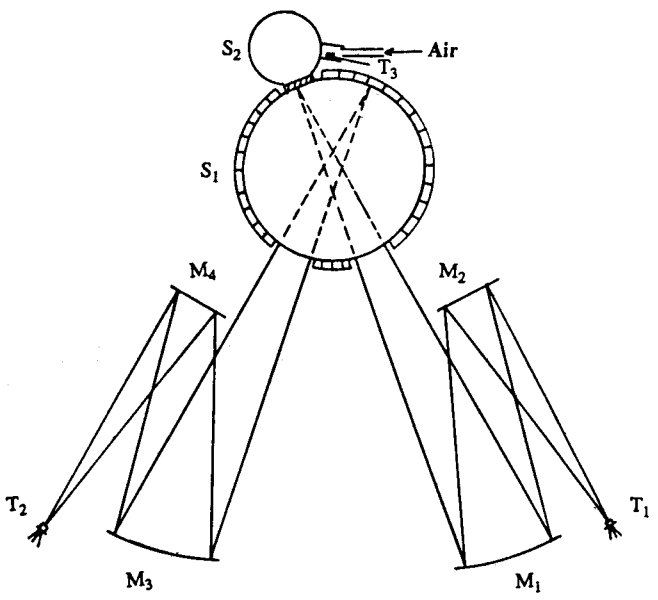

Fig. 2 Experimental setup.

sample is in contact with the port of an integrating sphere. This generates a diffuse boundary intensity on each side of the sample proportional to the respective exit flux. Multidimensional calculations of the radiative heat flux[21] indicate that the aspect ratio, port diameter to slab thickness, of the sample should be at least 6:1 to make the physical problem one-dimensional. The system was designed to minimize the cumulative system flux ratio losses.

The apparatus is modeled as having purely diffuse flux incident on both boundaries. Transmittance is referred to as sample transmittance because the measured quantity interacts mainly with the sample. Reflectance is referred to as system reflectance of the sample plus retransmitted radiation from an integrating sphere. Care was taken so that higher-order system interactions and problems with achieving a measurable signal did not affect the model. Briefly, this involved multidimensional analysis of the sample, considerable testing, and analysis of systems of integrating spheres, sources, and detectors, and finally test and analysis to assure that samples did not change temperature during the tests.

The radiative intensity at the initial boundary of the sample consists of the incident radiation plus successive interactions with the medium and the sphere. This may be modeled simply as the measured incident intensity a_1 on a transparent boundary. The radiative flux going back into the medium at the second boundary is proportional to that exiting because of the sphere. This may again be measured directly as a_2, assuming a diffuse boundary. The boundary conditions are therefore given by

$$I(0, \mu) \equiv a_1 \qquad \mu > 0 \tag{2}$$

$$I(\tau_0, \mu) = 2 \int_{\mu=0}^{1} I(\tau_0, \mu')\, \mu' \mathrm{d}\mu' = a_2 \qquad \mu < 0 \tag{3}$$

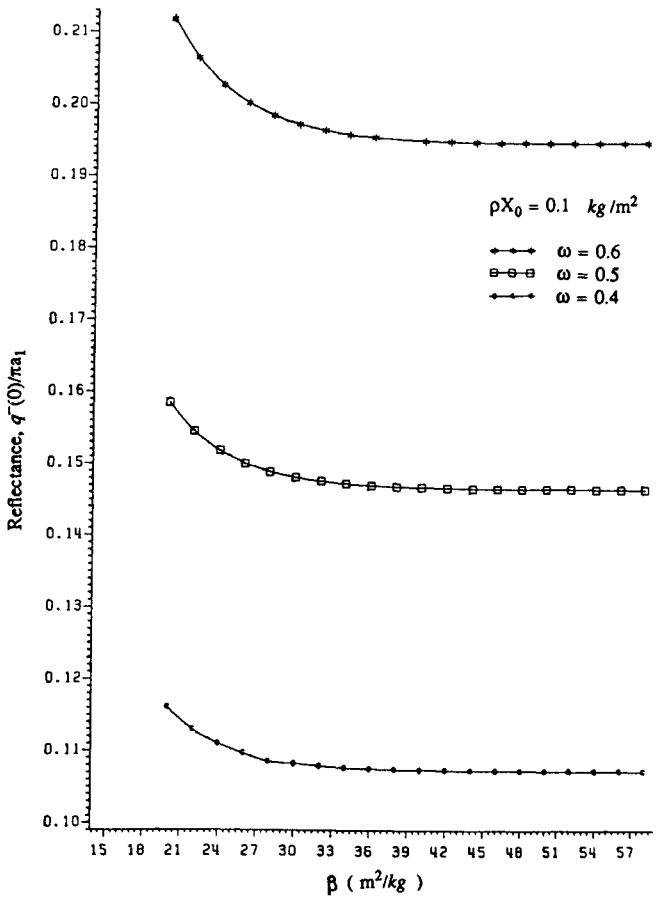

Fig. 3 Reflectance vs extinction coefficient.

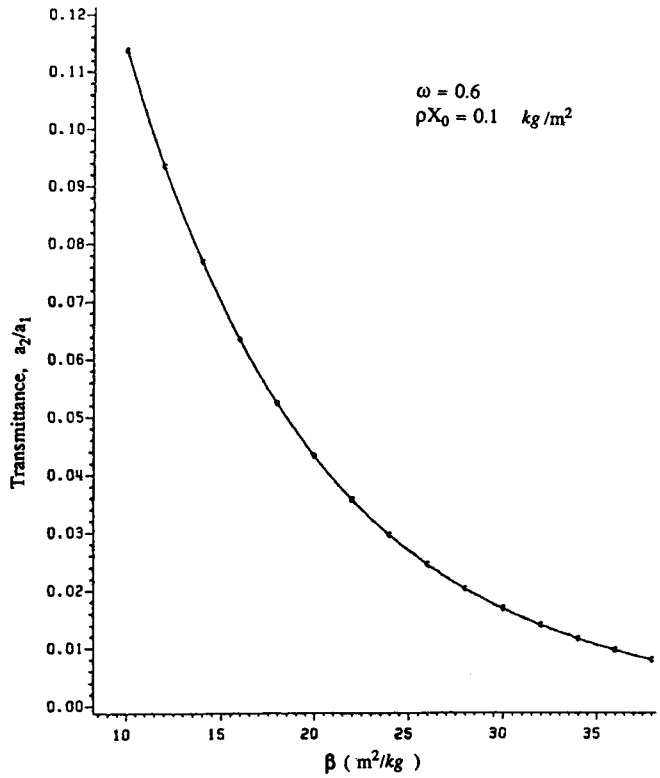

Fig. 4 Transmittance vs mass extinction coefficient.

The problem posed here by Eqs. (1-3) may be solved analytically using Case's normal mode expansion technique. The application of the method and results for hemispherical reflectivity are given in Chapter 11 of Ozisik.[22] That analysis and superpositioning[6] are applied to construct the theoretical results given in Figs. 1, 3, and 4. The separation of the variables solution generated by Case's technique is exact within the order of quadrature used to represent the continuum eigenvalues. Results in the figures presented here use an 80-point quadrature.[23] In order to solve Eq. (1), superpositioning is applied as follows:

$$I(\tau, \mu) = a_1 \psi_1(\tau, \mu) + a_2 \psi_2(\tau, \mu) \tag{4}$$

where ψ_1 and ψ_2 are the intensities defined by

$$\mu \frac{\partial \psi_1}{\partial \tau} + \psi_1 = \frac{\omega}{2} \int_{-1}^{1} \psi_1 \mathrm{d}\mu' \tag{5}$$

with the boundary conditions of

$$\psi_1^+(0, \mu) = 1 \tag{6}$$

$$\psi_1^-(\tau_0, \mu) = 0 \tag{7}$$

and

$$q_1^+(\tau_0) = 2\pi \int_{\mu=0}^{1} \psi_1^+(\tau_0, \mu')\mu' \mathrm{d}\mu' \tag{8}$$

$$q_1^-(0) = 2\pi \int_{\mu=0}^{1} \psi_1^-(0, \mu')\mu' \mathrm{d}\mu' \tag{9}$$

where q^+ and q^- are the fluxes at the boundaries, and

$$\mu \frac{\partial \psi_2}{\partial \tau} + \psi_2 = \frac{\omega}{2} \int_{-1}^{1} \psi_2 \mathrm{d}\mu' \tag{10}$$

with the boundary conditions of

$$\psi_2^+(0, \mu) = 0 \tag{11}$$

$$\psi_2^-(\tau_0, \mu) = 1 \tag{12}$$

and

$$q_2^+(\tau_0) = 2\pi \int_{\mu=0}^{1} \psi_2^+(\tau_0, \mu')\mu' d\mu' \tag{13}$$

$$q_2^-(0) = 2\pi \int_{\mu=0}^{1} \psi_2^-(0, \mu')\mu' d\mu' \tag{14}$$

Obviously, ψ_1 and ψ_2 are solutions to the same physical problem, but

$$q_1^+(\tau_0) = q_2^-(0) \tag{15}$$

and

$$q_1^-(0) = q_2^+(\tau_0) \tag{16}$$

For the transmittance part of the problem, operating on Eq. (4),

$$a_2 \equiv 2 \int_{\mu'=0}^{1} I^+(\tau_0, \mu')\mu' d\mu' \tag{17}$$

Equation (17) becomes

$$a_2 = 2a_1 \frac{q_1^+(\tau_0)}{2\pi} + 2a_2 \frac{q_2^+(\tau_0)}{2\pi}$$

Using Eq. (16), this reduces to

$$\pi a_2 = a_1 q_1^+(\tau_0) + a_2 q_1^-(0)$$

Thus,

$$a_2 = \frac{a_1 q_1^+(\tau_0)}{\pi - q_1^-(0)} \tag{18}$$

Since $q^+(\tau_0) = \pi a_2$, then

$$\pi a_2 = \frac{\pi a_1 q_1^+(\tau_0)}{\pi - q_1^-(0)} \tag{19}$$

$q_1^+(\tau_0)$ and $q_1^-(0)$ are determined from the singular eigenfunction expansion method based on the simple problem $\psi_1(\tau, \mu)$.

Introducing

$$\text{Reflectance} \equiv Re = \frac{q_1^-(0)}{\pi} \tag{20}$$

and

$$\text{Transmittance} \equiv Tr = \frac{q_1^+(\tau_0)}{\pi} \tag{21}$$

for our problem

$$\frac{a_2}{a_1} = \frac{q^+(\tau_0)}{q^+(0)} = \frac{[\pi a_1 q_1^+(\tau_0)]/[\pi - q_1^+(0)]}{\pi a_1} = \frac{q_1^+(\tau_0)}{\tau - q_1^-(0)}$$

or

$$\frac{a_2}{a_1} = \frac{Tr}{1 - Re} \tag{22}$$

Now, for the reflectance part of this problem, we need to calculate $[q^-(0)]/\pi a_1$, where

$$q^-(0) = 2\pi \int_{\mu=0}^{1} I^-(0, \mu')\mu' d\mu' \tag{23}$$

Using Eq. (4), Eq. (23) changes to

$$q^-(0) = 2\pi a_1 \int_{\mu=0}^{1} \psi_1^-(0, \mu')\mu' d\mu' + 2\pi a_2 \int_{\mu=0}^{1} \psi_2^-(0, \mu')\mu' d\mu' \tag{24}$$

Using Eqs. (9), (14), and (16), Eq. (24) reduces to

$$\frac{q^-(0)}{\pi a_1} = Re + \frac{a_2}{a_1} Tr \tag{25}$$

The calculated system reflectance, which is proportional to the ratio of the half-range negative radiative heat flux of the system to the incident flux, $[q^-(0)]/\pi a_1$, is plotted in Fig. 3 against β. Clearly, for large optical thickness $\rho X_0 \beta$, the albedo ω may be determined from the measured quantities, ρX_0 and $[q^-(0)]/\pi a_1$. With the albedo ω determined from the reflectance measurement, the transmittance may be used to determine the extinction coefficient β. The hemispherical transmittance measurement produces the ratio a_2/a_1, utilized in the analysis for this determination. If the transmittance and ρX_0 are known, β is uniquely determined. For example, Fig. 4 illustrates the theoretical variation of β as a function of this ratio for fixed values of $\omega = 0.6$ and $\rho X_0 = 0.001$ kg/m^2.

Experimental Measurement

The setup for this experiment is shown in Fig. 2. The apparatus includes two integrating spheres S_1 and S_2, front surface flat mirrors M_2 and M_4, front surface concave mirrors M_1, and M_3, and three thermopile detectors T_1, T_2, and T_3. The concave mirrors M_1 and M_3 are used to collect energy from the sample as well as the radiosity of sphere S_1 and focus the energy onto thermopiles T_1 and T_2. M_3 and M_4 are flat mirrors used to fold the beam onto the detectors. Transmittance is measured by detecting the radiosity from the surface of sphere S_2 with thermopile T_3.

Energy Source

The large sphere S_1 was used as a blackbody source of energy for the system. A 1/2-in. flexible heating tape, evenly spaced about the exterior, was used to heat the sphere. The tape was attached with a high-temperature, high-thermal-conductivity epoxy. Calculation indicates minimal temperature distribution about the sphere; six thermocouples were mounted on the surface to monitor the sphere temperature. The sphere was mounted on a wood stand in order to minimize the heat loss to the base, and 2 in. of glass-fiber insulation were used to cover the sphere so that the energy would be conserved inside the sphere. The internal part of the sphere was evenly roughened and painted with a very flat black paint. Hole sizes in this sphere were also minimized so that the sphere could be modeled as a blackbody source. Because all measurements were relative flux ratios, any errors from assuming a perfect blackbody are minor.

Spheres

The aluminum spheres used in the setup, Fig. 2, have diameters of 12 and 4-¾ in. The large sphere is fastened together by an aluminum ring using high-temperature, high-thermal-conductivity epoxy, and mounted on a wooden stand

that is fixed to the optical bench. The small sphere is assembled using flanges that are bolted to the vertical stand.

The large sphere has three 2-in.-diam holes. Two of them are used for detecting energy for reflectance measurements, and the third hole is used as a port for the samples. The small sphere has two holes; one serves as a port for the sample and the second hole as a window for detecting energy in transmittance measurements. This small sphere is uniformly roughened but unpainted.

Mirrors

Mirrors M_1 and M_3 are spherical 6-in.-diam, 32-in.-radius of curvature, first surface mirrors. Mirrors M_2 and M_4 are 4-in.-diam, flat, first surface mirrors. The concave mirrors are set up in such a way as to have the minimum amount of aberration; the maximum angle (angles between incident and reflected rays) is less than 15 deg. Also, the flat mirrors are arranged so that the angles are less than 90 deg between the incident and reflected ray.

Air System

Glass-fiber insulation will absorb a small amount of the incident radiant energy, and a temperature increase due to this absorption may be observed for long-term measurements. This increase in temperature can cause an increase in emitted energy and could result in a significant portion of the detected energy. In order to prevent this, a flow of air through fiberglass was provided through the 1-in. hole of sphere S_2, Fig. 2. The amount of air needed to cool the fiberglass was estimated, and measurement runs were made to be sure extraneous cooling did not affect the experiment.

Compressed air provided in the laboratory was passed through a regulator, an air drier, and an airflow meter. Air flowed through a sufficient length of hose to bring air to room temperature when it entered the sphere. This flow also prevented the long-term increase of the temperature of the small collecting sphere S_2.

Energy Detector

Thermopile detectors T_1, T_2, and T_3 (Fig. 2) used in the setup are Model M5 from Dexter Research Center. These were constructed using evaporated bismuth and antimony.[24] An energy-absorbing black paint or smoke is deposited on the junction area. The element is hermetically sealed in a TO-5 package under a purge atmosphere of argon or nitrogen. The spectral absorption of the deposited blacks are essentially flat from the ultraviolet to the far infrared. The windows on these were potassium bromide (KBr), which also has a transmission of at least 93% for wavelengths of 1–20 μm.

Glass-Fiber Insulation

Several different brands and manufacturing runs of glass-fiber insulation were used in this experiment. Three samples were chosen from each brand, with different thickness or ρX_0. Owing to random orientation and distribution of fibers, measurements were taken at five different locations on the samples, in order to determine average properties.

Samples were held by a ring and clamed in place with a precision-sized smaller ring inside it in order to minimize compression of the sample. The ring was in contact with the spheres, and efforts were made to reduce the transfer of heat by conduction. In order to accomplish this, the ring holding the specimen was machined from acrylic plastic.

Experimental Procedure

Because of the structure of fiber insulation and the indefinite irregular surface, it is difficult, if not impossible, to establish the density and thickness of small, thin samples. For this reason, the value of the product of these two properties is determined by measuring the area of the specimen and then weighing that specimen on an analytical balance. The mass of the specimen divided by the area gives the property ρX_0. Thus, since optical thickness is $\rho X_0 \beta$, a measurement of optical thickness permits the determination of the mass extinction coefficient β.

In this experiment, the albedo ω is first determined using the value of measured reflectance and the measured ρX_0 for the specimen. If the specimen is optically thick, Tr approaches 0 in Eq. 25. Utilizing the analytical solutions as plotted in Fig. 3, the value of ω may be determined uniquely from the measured reflectance. A solution for the problem using that albedo ω may then be determined for the known albedo and measured ρX_0 as demonstrated in the plot in Fig. 4. The transmittance of the specimen is measured and β determined uniquely from the solution for the given ω and ρX_0.

Results

Four different brands of glass-fiber insulation were chosen for our samples: Blodgett Market (yellow), Owens Corning (pink), Manville (yellow), and Wrap-On (yellow).

The complete data for Blodgett Market insulation are given in order to illustrate the range error in the current work. This particular brand of insulation had the widest range of variation; comments on the range of accuracy for several others are included. For complete details of all calculations or any minor instrumentation specification left out due to space limitations, see Saboonchi.[20]

Three samples of Blodgett Market insulation were constructed with weight densities ρX_0 of 2.0625×10^{-3}, 8.881×10^{-4}, and 5.913×10^{-4} kg/m^2. The optically thickest sample, $\rho X_0 = 2.0625 \times 10^{-3}$, allowed no transmittance. At the beginning of the reflectance tests for this sample, the room temperature was 22.2°C; during all tests, the experimental arrangement was isolated from room air conditioning/heating. The source sphere ranged from 72.3 to 75.2°C for this sample. The final room temperature was 22.6°C. As noted earlier, the sample and collecting sphere were maintained between 22.2 and 22.6°C during this process. Five voltage ratios directly corresponding to reflectance were measured in the range between 0.11494 and 0.16471. Using the analysis presented here, the calculated albedos ranged between 0.42 and 0.54, with an average of 0.51 and standard deviation of 0.045. The standard deviation for all other cases was typically between 2 and 7% of average property. With no measurable transmittance, no extinction coefficient could be determined for this sample.

For the same material with $\rho X_0 = 8.881 \times 10^{-4}$ kg/m^2, the average of five tests was 0.71 with a standard deviation of 0.019. The test source ranged from 74.2 to 75.9°C for reflectance and was uniform at 71.1°C for transmittance,

Table 1 Glass fiber insulations

Manufacturer	Color	ω_{avg}	β_{avg}, m^2/kg
Blodgett Market	Yellow	0.64	32.6
Owens Corning	Pink	0.73	36.2
Manville	Yellow	0.61	34.5
Wrap-On	Yellow	0.79	35.5
Average		0.69	34.7

Table 2 Ceramic fiber insulation

Fiberfrax Co.	ω	β, m^2/kg
Durablanket	0.93	38
Fiberfrax 110 paper	0.74	–
Fiberfrax cloth, tape, and sleeving	0.52	–

Table 3 Nonfibrous insulation

Manufacturer	Color	ω	β, m^2/kg
Insul Board Co.	White	0.76	34.7
Reeves Co.	Dark Gray	0.66	20.1

Table 4 Averaged mass extinction coefficients and albedos of glass-fiber insulation

Wavelength averaged	Current work	Love and Saboonchi[18] Saboonchi[19] 2.5–6μm	Tong and Tien[16] 2–4.5μm	Chan[2] 2.4–20μm	
	Experimental	Experimental	Experimental	Theoretical	Experimental
Mass extinction coefficient β, m^2/kg	34.7	37.4	209	99.5[a]	45.0[b]
Averaged albedo, ω_{avg}	0.69	–	0.597	–	–

[a]For glass fiber insulation with density 11.10 kg/m³. [b]For glass fiber insulation with density 9.93 kg/m³.

while the room ranged from 22.2 to 22.6°C during this sequence of tests. Both reflectance and transmittance were determined concurrently for a given sample. Here, the voltage ratio corresponding directly to transmittance ranged from 0.10000 to 0.11666. The analysis yields mass extinction coefficients (for known ρX_0 and albedos) of 30.1 to 32.8 m^2/kg, with an average of 31.3 and a standard deviation of 0.906.

Finally for $\rho X_0 = 5.913 \times 10^{-4}$, albedo ranged from 0.64 to 0.73, with an average of 0.69 and a standard deviation of 0.032 (74.2–75.9°C). Mass extinction coefficient ranged from 29.6 to 35.7, with an average of 33.8 and a standard deviation of 2.205 (71.2°C uniform). The ambient temperature before the tests was 22.2°C and was 22.6°C after the tests.

The entire sequence of tests were averaged to give the Table 1 values. Clearly, discarding the optically thick readings would give an albedo of 0.70, or about 10% higher than reported. For completeness, note that, for Owens Corning fiber insulation, the three test averages for albedo were 0.80, 0.71, 0.68 for weight densities of 2.261×10^{-3}, 8.885×10^{-4}, and 6.738×10^{-4}, respectively. Manville was the most consistent for the tests here, with albedos of 0.59, 0.61, and 0.64 for corresponding weight densities of 2.520×10^{-3}, 7.499×10^{-4}, and 6.539×10^{-3} kg/m^2. In Table 1, the average value of albedo and extinction coefficient are shown from three samples of each brand of fibrous insulation. The color is a visible indication and apparently did not have any effect on the infrared properties. The color is listed only as an aid in identifying the material.

In addition, three different types of insulation from Fiberfrax Company were chosen to measure radiative properties ω and β:

1) Durablanket (white), which is a lightweight, flexible needled blanket made from long Fiberfrax ceramic fibers. In this material, since the fibers were not in layers, it was very difficult to have a uniform sample. Therefore, there is a larger variation on the measured values of reflectance than in the glass-fiber insulation.

2) Fiberfrax 110 Paper, which is a rigid paper. For this insulation, it was difficult to cut a thin sample and it was not possible to obtain a measurable value for transmittance.

3) Fiberfrax cloth, tape, and sleeving. This cloth was also optically thick, and it was not possible to obtain a reasonable value for transmittance.

In Table 2, the values for average β and ω are given for Fiberfrax Company material.

In addition to the values in Table 2, measurements were also made on styrofoam. The specimen, Type M insulative sheeting of expanded polystyrene (EPS), was obtained from the Insul Board Company. This material had a higher value of transmittance relative to others. Foam insulation from Reeves Company was also chosen for measurement of radiative properties. This material is primarily used for automotive insulation and has a very uniform density. Table 3 gives the average value for ω and β of styrofoam and sponge foam insulation.

In Table 4, the results of these experiments have been compared with the results of other investigators. Tong and Tien[16] present values approximately two times larger than the present results. Chan[19] published results 1.5–3 times larger than the present measurements. Love and Saboonchi[18] and Saboonchi[19] previously reported results in which Beer's law was used to calculate β. Those findings were only slightly larger than the results of the present study.

Conclusions

The present work presents a method for the unique determination of ω and β based on an isotropic gray model. It is argued that for most engineering computations of radiative heat transmission, this model is the most practical because the directional spectral properties of the boundary materials are seldom known for an enclosed insulated space. The majority of all radiative computations assume gray diffuse surfaces, and practical considerations suggest that the assumed model will be of wide benefit.

The properties given will permit analysis of combined radiative and conductive analysis for heat transfer through insulated spaces. Future work will develop spectral properties using a similar experimental method with wavelength discrimination. This should improve predictions of radiative heat transfer through insulated space at relatively large absolute temperature differences.

Acknowledgments

This work was partially sponsored by a grant from the University of Oklahoma Research Council and by National Science Foundation Grant CBT 85 06510.

References

[1]Pelanne, C.M. "Heat Flow Principles in Thermal Insulation," *Journal of Thermal Insulation,* Vol. 1, July 1977, pp. 48–80.

[2]Chan, F.F., "Energy Transfer in Fibrous Insulating Materials," M.S. Thesis, Univ. of Kentucky, Lexington, 1979.

[3]Hager, N.E. and Steere, R.C., "Radiant Heat Transfer in Fibrous Thermal Insulation," *Journal of Applied Physics,* Vol. 38, Nov. 1967, pp. 4663–4668.

[4]Hottel, H.C., Sarofim, A.F., Evans, L.B., and Vasolos, I.A., "Radiative Transfer in Anisotropically Scattering Media: Allowance for Fresnel Reflection at the Boundaries," *Journal of Heat Transfer,* Vol. 90, Feb. 1968, pp. 56–62.

[5]Larkin, B.K. and Churchill, S.W., "Heat Transfer by Radiation Through Porous Insulation," *AIChE Journal,* Vol. 5, Dec. 1959, pp. 467–474.

[6]Ozisik, M.N. and Sutton, W.H., "Source Function Expansion in Radiative Transfer," *Journal of Heat Transfer,* Vol. 102, Nov. 1980.

[7]Rish, J.W. and Roux, J.A., "Heat Transfer Analysis of Fiberglass Insulations With and Without Foil Radiant Barriers," *Journal of Thermophysics and Heat Transfer,* Vol. 1, Jan. 1987.

[8]Roux, J.A., Todd, D.C., and Smith, A.M., "Radiative Transfer with Anisotropic Scattering and Arbitrary Temperature for Plane Geometry," *AIAA Journal,* Vol. 16, Sept. 1973, pp. 1203–1211.

[9]Roux, J.A. and Smith, A.M., "Combined Conduction and Radiation Heat Transfer in an Absorbing and Scattering Medium," *Journal of Heat Transfer,* Vol. 100, Feb. 1978, pp. 98–104.

[10]Roux, J.A., Yeh, H.Y., Smith, A.M., and Wang, S.Y., "Finite Element Analysis of Radiative Transport in Fibrous Insulation."

AIAA Paper 83-1502, June 1983; also *Journal of Energy,* Vol. 7, Nov.-Dec. 1983, pp. 702-709.

[11]Tong, T.W. and Tien, C.L., "Analytical Model for Thermal Radiation in Fibrous Insulation," *Journal of Thermal Insulation,* Vol. 4, July 1980, pp. 27-44.

[12]Tong, T.W. and Tien, C.L., "Radiative Heat Transfer in Fibrous Insulation – Part I: Analytical Study," American Society of Mechanical Engineers Paper 81-HT-42, Aug. 1981.

[13]Verschoor, J.D. and Greebler, P., "Heat Transfer by Gas Conduction and Radiation in Fibrous Insulation," *Transactions of ASME,* Vol. 74, Aug. 1952, pp. 961-968.

[14]Wolf, P., "An Analytical and Experimental Study of the Radiative Heat Transfer in Scattering, Absorbing, and Emitting Media," Ph.D. Dissertation, Univ. of Knoxville, Tennessee, 1968.

[15]Yuen, W.W. and Wong, L.W., "Heat Transfer by Conduction and Radiation in a One-Dimensional Absorbing, Emitting and Anisotropically Scattering Medium," *Journal of Heat Transfer,* Vol. 102, May 1980, pp. 303-307.

[16]Tong, T.W., Yang, Q.S., and Tien, C.L., "Radiative Heat Transfer in Fibrous Insulation – Part II: Experimental Study," American Society of Mechanical Engineers Paper 81-HT-43, Aug. 1981.

[17]Tong, T.W., Liu, W.L., and Subramanian, E., "The Effect of Multiple Scattering in Measuring the Radiation Properties of Absorbing and Scattering Media," AIAA Paper 83-1454, June 1983.

[18]Love, T.J. and Saboonchi, A., "Determination of the Extinction Coefficient of Glass Fiber Insulation," AIAA Paper 80-1528, 1980.

[19]Saboonchi, A., "Determination of the Extinction Coefficient of Glass Fiber Insulation," M.S. Thesis, Univ. of Oklahoma, Norman, 1979.

[20]Saboonchi, A., "A Method for the Determination of Thermal Radiation Properties of Fiber Insulation," Ph.D. Dissertation, Univ. of Oklahoma, Norman, 1986.

[21]Sutton, W.H. and Ozisik, M.N., "An Alternative Formulation for Radiative Transfer in an Isotropically Scattering Two-Dimensional Bar Geometry and Solution Using the Source Function Expansion Method," American Society of Mechanical Engineers Paper 84-HT-36, Aug. 1984.

[22]Ozisik, M.N., *Radiative Transfer,* Wiley, New York, 1973.

[23]Abramowitz, M. and Stegin, I.A., (eds.), *Handbook of Mathematical Functions,* Dover, New York, 1972.

[24]Data Sheets, Model M5 Detector, Technical Description, Dexter Research Center, Dexter, MI, Oct. 1980.